



Novel quinoxaline derivatives containing arylaminated aceanthrylene for organic red-light emitting diodes

Jae-Wan Jang^b, Hyuntae Park^a, Min-Ki Shin^b, Hyeon Hui Kang^a, Dae-Hwan Oh^a,
Sung Ouk Jung^c, Soon-Ki Kwon^{b,*}, Yun-Hi Kim^{a,*}

^aDepartment of Chemistry and RINS, Gyeongsang National University, Jinju 660-701, South Korea

^bSchool of Materials Science and Engineering and ERI, Gyeongsang National University, Jinju 660-701, South Korea

^cSFC Co., LTD., Cheongwon 363-883, South Korea

ARTICLE INFO

Article history:

Received 26 November 2009

Received in revised form

26 April 2010

Accepted 26 April 2010

Available online 4 May 2010

Keywords:

Quinoxaline derivatives

Arylaminated aceanthrylene

Organic light emitting diodes

Red emission

Thermal stability

Efficiency

ABSTRACT

Novel quinoxaline derivatives containing arylaminated aceanthrylene, *N,N*-diphenylaceanthryleno[2,1-*b*]quinoxalin-5-amine and *N*-(naphthalen-2-yl)-*N*-phenylaceanthryleno[2,1-*b*]quinoxalin-5-amine, were synthesized as red light emitting materials for use in organic light emitting diodes. The synthesized materials showed good thermal stability with glass transition temperatures of 142 °C for *N,N*-diphenylaceanthryleno[2,1-*b*]quinoxalin-5-amine and 163 °C for *N*-(naphthalen-2-yl)-*N*-phenylaceanthryleno[2,1-*b*]quinoxalin-5-amine. The dipolar characteristic of the quinoxaline derivatives resulted in prominent solvatochromic effects. The fabricated devices based on *N,N*-diphenylaceanthryleno[2,1-*b*]quinoxalin-5-amine showed maximum brightness of 17 523 cd/m² and current efficiency of 4.55 cd/A with chromaticity coordinates of 0.56 and 0.43. Devices based on *N*-(naphthalen-2-yl)-*N*-phenylaceanthryleno[2,1-*b*]quinoxalin-5-amine containing *N*-naphthyl-*N*-phenyl amine displayed red emission (*x*, *y* = 0.60, 0.39) with maximum brightness of 4239 cd/m² and current efficiency of 2.76 cd/A. The results show that the synthesized quinoxaline derivatives offer promise as materials for stable and efficient red emitting organic light emitting diodes.

© 2010 Elsevier Ltd. All rights reserved.

1. Introduction

During the past two decades, much research and development has attended organic light emitting diodes (OLEDs). Owing to their wide range of emission colours, high brightness, low cost and low power consumption, OLEDs have potential as 'next generation' full-color flat-panel displays. To realize a vivid full-color display, pure red, green and blue organic light emitters of high efficiency, appropriate chromaticity coordinates and luminescence are required [1]. Among the various organic light emitters, blue and green light emitting materials have been developed in order to meet the requirements for commercialization of OLEDs. Numerous electro-phosphorescent and electrofluorescent blue and green light emitting materials have been reported to date [2–9]. However, the red-light emitting OLEDs remain inefficient for the realization of such next generation full-color displays because of their low efficiency, low stability and low color purity. Red emitting organic materials have a narrow band gap between the highest occupied molecular orbital (HOMO) and the

lowest unoccupied molecular orbital (LUMO) and display low efficiency due to the non-radiative relaxation of the excited state [1]. Moreover, they have strong intermolecular dipole–dipole interactions or intermolecular π -stacking characteristics owing to their polar or extensively π -conjugated structures. This results in a tendency to aggregate, giving rise to concentration quenching [1,10–12]. The synthesis of many red emitting materials is a complicated process of low yield [13].

The majority of organic red emitting electroluminescent materials were designed on the basis of electron-donating and electron-withdrawing groups within a conjugated system or Eu³⁺ based complexes [14–17]. The widely used red emitting materials contain – pyran group such as 4-(dicyanomethylene)-2-methyl-6-(*p*-dimethylaminostyryl)-4H-pyran (DCM1), 4-(dicyanomethylene)-2-methyl-6-(julolidin-4yl-vinyl)-4H-pyran (DCM2), 4-dicyanomethylene-2-methyl-6-(1,1,7,7-tetramethyljulolidyl-9-enyl)-4H-pyran (DCJT) and 4-(dicyanomethylene)-2-*t*-butyl-6-(1,1,7,7-tetramethyljulolidyl-9-enyl)-4H-pyran (DCJTb). These have been used in conjunction with congeners [1] in which julolidin groups were utilized as electron donors and cyano groups as electron-withdrawing groups. Although these materials have been reported as red-emitters, their reported color in

* Corresponding authors.

E-mail addresses: skwon@gnu.ac.kr (S.-K. Kwon), ykim@gnu.ac.kr (Y.-H. Kim).

terms of the EL spectrum complicates estimations of their color purity levels [1]. Recently, several groups have reported quinoxaline derivatives as electron transporting and/or hole transporting materials in OLEDs [18–22]; however, these have low efficiency and chemical stability. It has been reported that anthracene has interesting photo and electroluminescent properties and good electrochemical properties [23–30].

This paper concerns novel, red emitting materials composed of quinoxaline and aceanthrylene with triarylamine, QAD-I and QAD-II. The quinoxaline moiety increased the electron affinity (EA) of the molecules due to the additional imine nitrogen in the ring and improved both electron injection and transport properties [18,22]. Moreover, the introduction of aceanthrylene with an arylamine moiety increased efficiency not only owing to the anthracene unit having interesting photo and electroluminescent properties and good electrochemical and thermal properties, but also due to the arylamine unit that was utilized as an electron-donating group on the aromatic rings, as these are widely used as a hole-transporting layer. OLEDs based on synthesized quinoxaline derivatives were fabricated and the electroluminescent characteristics of devices based on novel QAD-I and QAD-II were also reported.

2. Experimental

All reagent and solvents used in this study were purchased from Aldrich Chemical Co. and Fluka. Only analytical grade quality chemicals were used for the experiments. Spectroscopic grade CHCl_3 (Aldrich) was used to measure UV–Visible absorption and emission spectra of the samples. Infrared (IR) spectra of materials synthesized were recorded using a Genesis II FT-IR spectrometer. ^1H NMR spectra were recorded using DRX 300 MHz NMR Bruker spectrometers and chemical shifts in the spectra are reported in units of parts per million with tetramethylsilane as internal standard. Thermogravimetric analyzer (TGA) of the samples were carried out using TA instrument 2050 thermogravimetric analyzer under nitrogen with heating rate of $10\text{ }^\circ\text{C}/\text{minute}$ from 50 to $800\text{ }^\circ\text{C}$. Differential scanning calorimetry (DSC) study was carried out for the samples using TA Instruments 2100 differential scanning calorimeter under nitrogen with heating rate of $10\text{ }^\circ\text{C}/\text{min}$ from 30 to $300\text{ }^\circ\text{C}$. A Jeol JMS-700 mass spectrometer was utilized to obtain

the mass spectra of the samples. UV–Vis absorption and photoluminescence (PL) spectra were recorded using Perkin–Elmer LAMBDA-900 UV–vis–NIR spectrophotometer and LS-50B luminescence spectrophotometer respectively. Cyclic voltammograms of samples were recorded at room temperature using epsilon E3 cyclic-voltmeter in a 0.1 M solution of tetrabutylammonium perchlorate (Bu_4NClO_4) in acetonitrile under the nitrogen environment at a scan rate of 50 mV/s. The platinum rod and wire were used as working and the counter electrode and a Ag/AgNO_3 electrode as the reference electrode.

Pre-patterned indium tin oxide (ITO) substrates were cleaned by sonication in a detergent solution for 2 min and then washed with a large amount of doubly distilled water. Further sonication in ethanol for 2 min was done before blowing dry with a stream of nitrogen. The ITO substrates were then treated with O_2 plasma for 1 min before being loaded into the vacuum chamber. The organic layers were deposited thermally at a rate of $0.1\text{--}0.3\text{ nm s}^{-1}$ under a pressure of about 10^{-6} torr. OLEDs devices were constructed with 20 nm of copper phthalocyanine (CuPc) (as the hole injection layer, 50 nm of 4,4'-bis[1-naphthylphenylamino]triphenylamine (NPB) as the hole-transporting layer, 20 nm of QAD-I or QAD-II (3 wt% in Alq_3) as the emission layer, 40 nm of Alq_3 as the electron transporting emission layer, 1 nm of LiF as the electron injection layer and 150 nm of Al as the cathode. The EL was measured under ambient conditions.

2.1. Synthesis of aceanthrylene-1,2-dione (1)

This compound was prepared from oxalyl chloride and anthracene by the reported procedure (mp = $268\text{ }^\circ\text{C}$) [31].

2.2. Synthesis of 6-bromo-aceanthrylene-1,2-dione (2)

A solution of **1** (5.4 g, 23.25 mmol) in nitrobenzene was heated to $145\text{ }^\circ\text{C}$ and stirred while a solution of bromine (3.90 g, 24.40 mmol) in nitrobenzene was added dropwise. The ensuing mixture was stirred and heated for 15 min, then cooled and diluted with ethanol to facilitate filtration. After washing with alcohol and drying, the yellow solid was obtained by crystallization from *o*-dichlorobenzene as reported (dp g; $260\text{ }^\circ\text{C}$) [32].

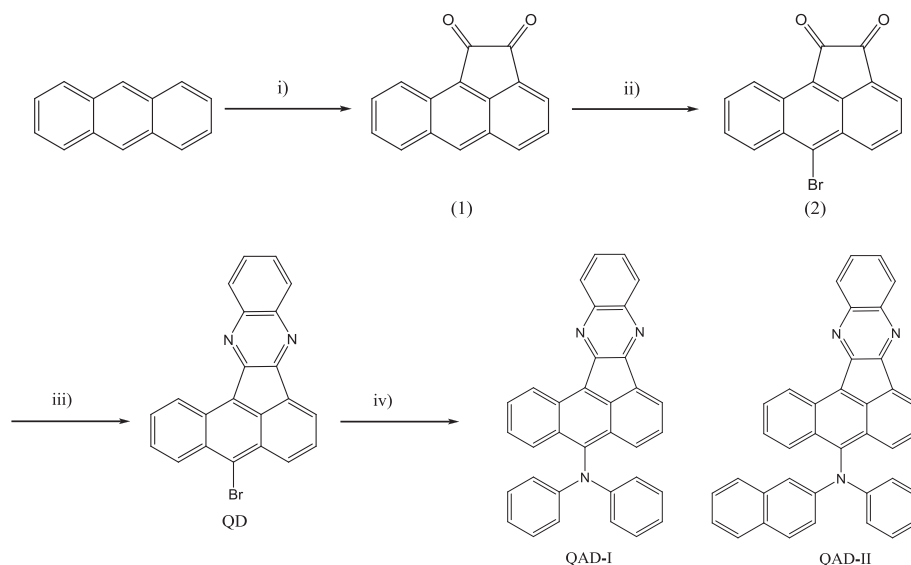


Fig. 1. Synthetic scheme of the quinoxaline derivatives of QAD-I and QAD-II: (i) oxalyl chloride, AlCl_3 , CS_2 , (ii) Br_2 , nitrobenzene, (iii) *o*-phenylenediamine, EtOH and (iv) $\text{Pd}(\text{OAc})_2$, $\text{P}(t\text{-Bu})_3$, NaO-*t*-Bu.

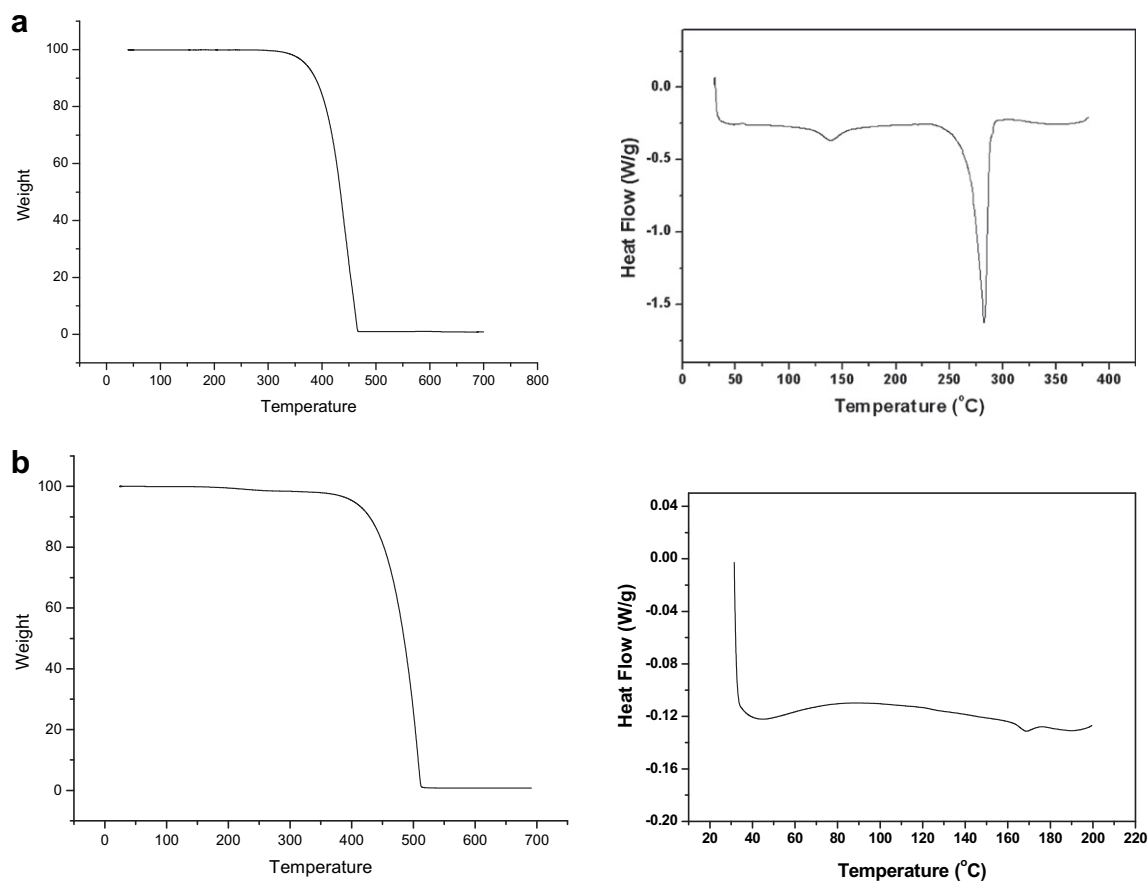


Fig. 2. The TGA and DSC curves of (a) QAD-I and (b) QAD-II.

2.3. Synthesis of quinoxaline derivative compound (QD)

This compound was prepared by the rapid condensation of *o*-phenylenediamine with **2** in boiling pyridine to give the quinoxaline derivative which was crystallized using chlorobenzene to provide a bright yellow solid (mp = 289 °C) [32].

2.4. Synthesis of quinoxaline derivative of QAD-I

A mixture of QD (2 g, 5.22 mmol), diphenylamine (1.06 g, 6.16 mmol), Pd(OAc)₂ (0.07 g, 0.1 mmol), tri-*tert*-butylphosphine (0.05 g, 0.26 mmol) and sodium *tert*-butoxide (0.75 g, 7.83 mmol) in toluene (30 mL) was stirred under nitrogen at 120 °C for 16 h. The ensuing mixture was allowed to cool to room temperature, filtered through cellite and washed with dichloromethane. The filtrate and washings were collected and washed with water and then dried over MgSO₄. The solvent was removed and the solid purified using silica gel column chromatography employing dichloromethane and hexane (3:1). Yield: 1.88 g (76.4%). ¹H NMR (300 MHz, CDCl₃): δ[ppm] = 8.46(d, 1H, 6.6Hz), 8.43–8.31 (m, 3H), 8.19 (d, 1H,

8.7Hz), 7.82–7.77 (m, 3H), 7.72–7.70 (m, 1H), 7.58–7.49 (m, 1H), 7.28–7.21 (m, 5H), 7.17–7.14 (m, 4H), 6.99–6.95 (m, 2H). FT-IR (KBr, cm⁻¹): 3030 (aromatic C–H), 1587 (C=N), 1542, 1495 (C=C), 1335 (C–N). Mass spectrometry (GC–MS): calcd for C₃₄H₂₁N₃: 473.19, found 473.19. Anal. calcd for C₃₄H₂₁N₃: C, 86.60; H, 4.49; N, 8.91, found: C, 86.56; H, 4.52, N, 8.83.

2.5. Synthesis of quinoxaline derivative of QAD-II

A mixture of QD (2 g, 5.22 mmol), naphthylphenylamine (1.34 g, 6.16 mmol), Pd(OAc)₂ (0.07 g, 0.1 mmol), tri-*tert*-butylphosphine (0.05 g, 0.26 mmol) and sodium *tert*-butoxide (0.75 g, 7.83 mmol) in toluene (30 mL) under a nitrogen atmosphere was stirred at 120 °C for 10–16 h. The mixture was allowed to cool to room temperature, filtered through cellite and washed with dichloromethane. The filtrate and washings were collected and washed with water and then dried over MgSO₄. The solvent was removed and the solid purified with silica gel column chromatography using dichloromethane and hexane (3:1). Yield: 1.96 g (72.2%). ¹H NMR (300 MHz, CDCl₃) δ[ppm] = 8.39–8.34 (m, 3H), 8.19–8.17 (m, 2H),

Table 1
Physical properties of quinoxaline derivatives.

Compound	T _m (°C) ^a	T _g (°C) ^a	HOMO (eV) ^b	LUMO (eV) ^b	CH ₂ Cl ₂ λ _{abs max} (nm)	<i>n</i> -Hexane λ _{em max} (nm)	Toluene λ _{em max} (nm)	EA λ _{em max} (nm)	THF λ _{em max} (nm)	CH ₂ Cl ₂ λ _{em max} (nm)
QAD-I	280	142	5.4	3.24	514	555	591	610	616	623
QAD-II	–	163	5.38	3.26	522	564	602	633	633	638

^a Melting and glass transition temperature (T_m, T_g) obtained from DSC measurement.

^b HOMO and LUMO measured in a CH₂Cl₂ solution. EA: Ethylacetate, THF: Tetrahydrofuran.

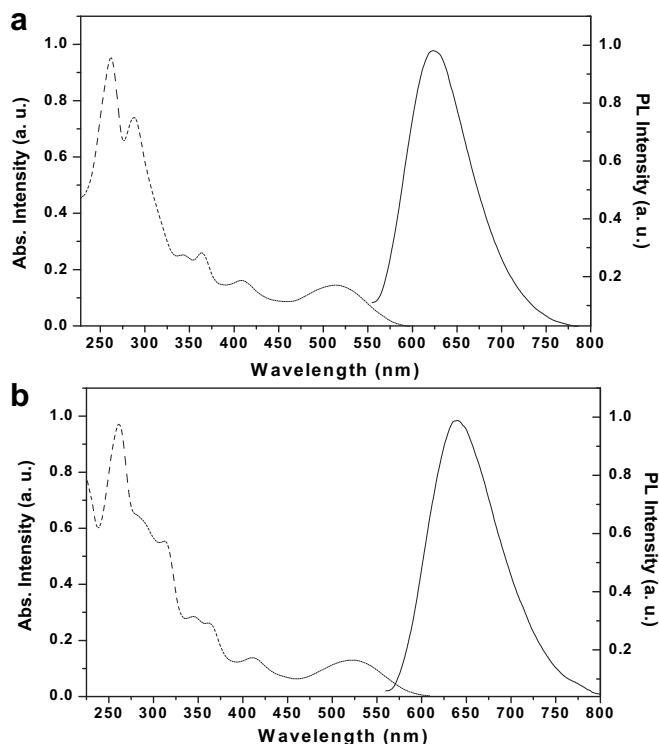


Fig. 3. UV–Vis absorption and photoluminescence spectra of (a) QAD-I and (b) QAD-II in CH_2Cl_2 .

7.79–7.74 (m, 5H), 7.62 (m, 1H), 7.52–7.50 (m, 3H), 7.35–7.25 (m, 8H), 7.04–6.98 (m, 1H). FT-IR (KBr, cm^{-1}): 3030 (aromatic C–H), 1585 (C=N), 1540, 1495 (C=C), 1338 (C–N). M ass spectrometry (GC–MS): calcd for $\text{C}_{38}\text{H}_{25}\text{N}_3$: 523.20, found: 523.20. Anal. calcd for $\text{C}_{38}\text{H}_{25}\text{N}_3$: C, 87.16; H, 4.81; N, 8.02, found: C, 87.20; H, 4.83; N, 8.11.

3. Result and discussion

The synthetic scheme of the novel organic materials, QAD-1 and QAD-II, is shown in Fig. 1. QAD-1 and QAD-II were easily synthesized by N-arylation of naphthylphenylamine or diphenylamine with 6'-bromo-aceanthrylene-1,2-quinoxaline obtained by the dehydration of 6'-bromoaceanthrylene-1,2-dione and phenylenediamine. After purification of the product by silica gel column chromatography, QAD-1 and QAD-II were obtained in the form of an orange solid with good yields of 76% and 72% respectively.

Compared with well known pyran-containing red dyes, the synthesized QAD-1 and QAD-II are more promising for the red emitting OLEDs because of their simple synthesis with high yield. The synthesized QAD-I and QAD-II were confirmed by various spectroscopic studies such as ^1H NMR, FT-IR, MS and elemental analysis. They exhibit good solubility in common organic solvents of dichloromethane, chloroform, toluene and o-dichlorobenzene despite the fact they have a fused planar system of aceanthryl-quinoxaline. The good solubility of QAD-1 and QAD-II could be due to the introduction of arylamine moiety.

The thermal behavior of QAD-1 and QAD-II was determined by thermogravimetric analyzer (TGA) and differential scanning calorimetry (DSC). QAD-1 and QAD-II show good thermal stability with the glass transition temperature (T_g) of 142 °C for QAD-I and 163 °C for QAD-II (Fig. 3). QAD-1 and QAD-II containing an aceanthryl group have increased T_g when compared to those containing an acenaphthyl group [18]. QAD-II with the N-naphthyl-N-phenyl amine shows a higher T_g than QAD-I with the N,N-diphenyl amine. The increased stability of the glassy state in these molecules can be due to the rigid fused aromatic structure and hence this can increase device longevity. In TGA studies, the 5% weight loss was observed at 405 °C for QAD-I and 453 °C for QAD-II (Fig. 3).

Fig. 2 shows UV–Vis absorption and PL spectra of QAD-1 and QAD-II in CH_2Cl_2 solution. The electronic spectra of the molecules reveal several bands arising from $\pi \rightarrow \pi^*$ and charge-transfer transitions. In particular, $\pi \rightarrow \pi^*$ transition of the characteristic anthracene and quinoxaline appeared at 335, 360, and 405 nm. The lower energy transition representing positive solvatochromism was considered mainly to be charge-transfer transition character. As the polarity of the solvent increased, the transition became red shifted. The UV–Vis absorption spectra of QAD-I and QAD-II show an absorption maximum at 514 nm for QAD-I and 522 nm for QAD-II. The fluorescence emission of QAD-I and QAD-II in various solvents are summarized in Table 1. Bathochromic shifts in the emission (for QAD-I and QAD-II) were observed in n-hexane (555 nm, 564 nm), toluene (591 nm, 602 nm), EA (610 nm, 633 nm) and THF (616 nm, 633 nm) as given in Table 1. QAD-1 and QAD-II containing aceanthryl group show more red-shift in UV–Vis absorption and emission when compared to those with an acenaphthyl group [18]. The emission maximum (λ_{max}) of QAD-II with an N-naphthyl-N-phenyl amine group is red-shifted when compared to that of QAD-I with an N,N-diphenyl amine group.

The electrochemical properties of the QAD-1 and QAD-II were investigated by cyclic voltammetric studies and the redox potentials of the compounds were assessed as shown in Table 1. QAD-I and QAD-II show reversible oxidation potentials characterized by E_{onset} value at 1.0 V and 0.98 V respectively. This is attributed to the

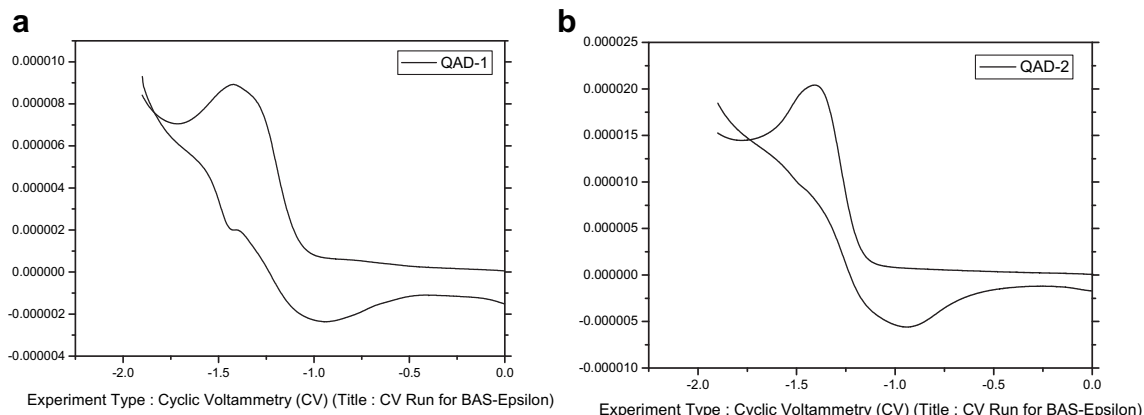


Fig. 4. The cyclic voltammetry of (a) QAD-I and (b) QAD-II.

oxidation of triphenylamine moiety. The estimated ionization potentials ($IP = E_{\text{onset}} + 4.4 \text{ eV} = \text{HOMO level}$) are about 5.4 eV for QAD-I and 5.38 eV for QAD-II. The higher HOMO energy levels of QAD-I and QAD-II can be efficient for the hole injection and transport. QAD-I and QAD-II also show the reduction potential (Fig. 4). The LUMO levels were approximately 3.24 and 3.26 eV for QAD-I and QAD-II respectively. QAD-I and QAD-II with the quinoxaline moiety show the lower LUMO levels, which will be much effective for the efficient electron injection and transport. These results suggest that QAD-I and QAD-II are more promising materials for the efficient red emitting OLED devices.

OLEDs based on QAD-I and QAD-II were fabricated using the configuration: indium tin oxide (ITO)/copper phthalocyanine (CuPc)/N,N-bis-(1-naphthalenyl)-N,N-bis-phenyl-(1,1-biphenyl)-4,4-diamine (NPB)/tris-8-hydroxyquinoline)aluminum (Alq_3): QAD-I (3 wt%) or QAD-II (3 wt%)/LiF/Al. CuPc, NPB, Alq_3 , LiF and Al layers were used as hole injection, hole transporting, electron transporting, electron injection and cathode layers respectively. QAD-I (3 wt%) doped in Alq_3 (host) for Device I and QAD-II (3 wt%) doped in Alq_3 for Device II were used as emissive layer (EML). As the color of fabricated devices with red dopant depends on the concentration of the dopants employed, OLEDs with red dopant (QAD-I for device I and QAD-II for device II) concentration of 3 wt% were fabricated for the improved

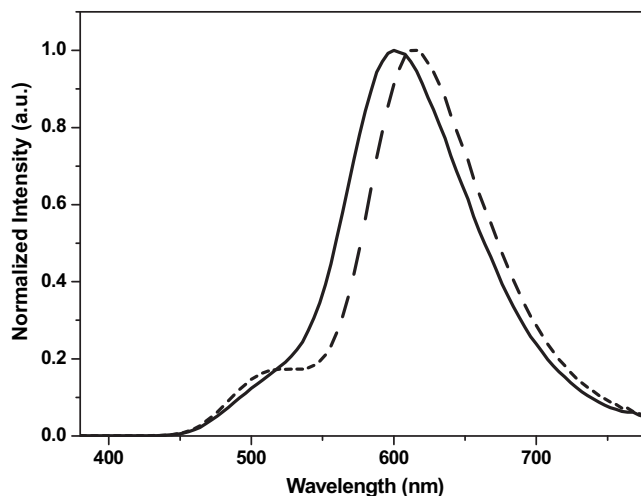


Fig. 6. Electroluminescence (EL) spectra of (—) device I and (---) device II.

performances. The voltage-luminance-efficiency characteristics are shown in Fig. 3. The maximum brightness and efficiency of device I were observed to be 17 523 cd/m^2 (7.78 V) and 4.55 cd/A (4.02 V) respectively. In the case of device II, the maximum brightness and efficiency were observed as 4239 cd/m^2 (8.6 V) and 2.76 cd/A (4.27 V) respectively. Hence, it is reported that the diphenylamino moiety in QAD-I gives higher brightness and efficiency in device I when compared to those of QAD-II with naphthyl phenyl amine in device II. The results suggest that the electron injection into QAD-I containing N,N-diphenyl amine moiety in device I can be improved when compared to that into QAD-II containing N-naphthyl-N-phenyl amine moiety in device II. The electroluminescence (EL) spectra of the devices I and II are shown in Fig. 5. In the EL spectra, it is confirmed that the emission comes from QAD-I and QAD-II due to efficient energy transfer from Alq_3 host although slight shoulder emission is represented in the 510 nm. It confirms that the introduction of acanthryl-quinoxaline derivatives causes a bathochromic shift in the EL spectrum. The observed EL spectra show a peak at 600 nm (CIE x,y: 0.56, 0.43) for device I and a peak at 616 nm (CIE x,y: 0.60, 0.39) for device II (Fig. 6).

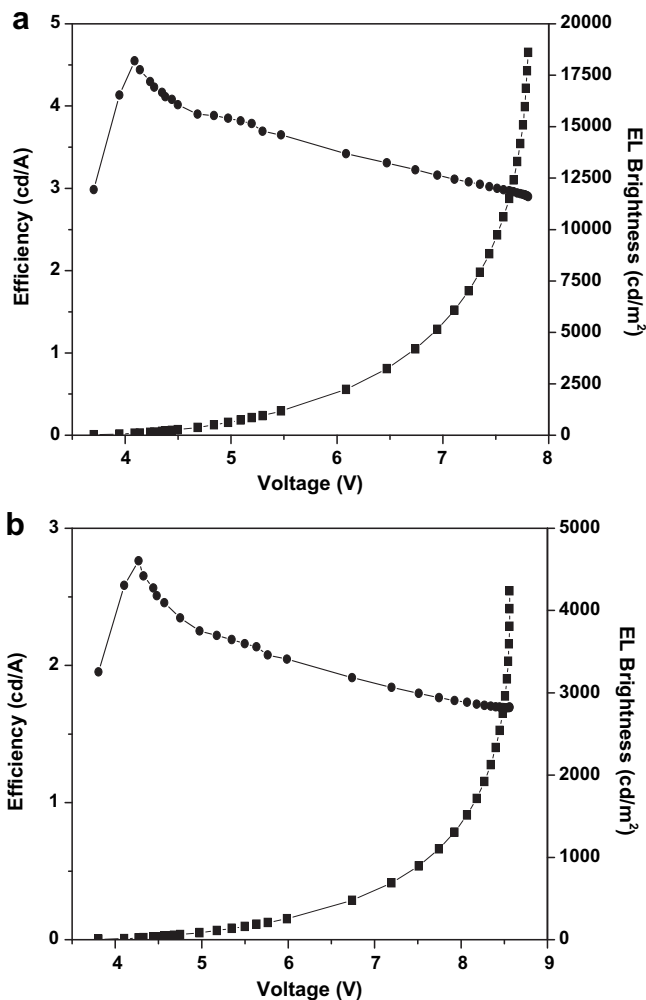


Fig. 5. Efficiency (●) – voltage – EL brightness (■) characteristics of (a) device I: ITO/CuPc/NPB/ Alq_3 : QAD-I (3 wt%)/LiF/Al and (b) device II: ITO/CuPc/NPB/ Alq_3 : QAD-II (3 wt%)/LiF/Al.

4. Conclusions

Novel quinoxaline derivatives containing arylaminated acanthrylene, QAD-I and QAD-II, were designed and synthesized successfully as red emitting materials in OLEDs. The quinoxaline moiety and arylamine group were utilized as the electron-withdrawing group and electron-donating group respectively in these derivatives. The introduction of anthracene leads to the improved color purity and thermal stability. When OLEDs based on these derivatives were fabricated, the characteristic electroluminescence (EL) spectrum of the device based on QAD-I containing N,N-diphenyl amine is observed at 600 nm (CIE: 0.56, 0.43) with a maximum brightness of 17 523 cd/m^2 (7.78 V) and efficiency of 4.55 cd/A (4.02 V). Devices based on QAD-II containing N-naphthyl-N-phenyl amine show the red emission at 616 nm (CIE: 0.60, 0.39) with the maximum brightness of 4239 cd/m^2 (8.6 V) and efficiency of 2.76 cd/A (4.27 V). It is proposed that the optimized device structures based on these novel quinoxaline derivatives, QAD-I and QAD-II, can be useful for the stable and efficient red emitting device applications.

Acknowledgments

The financial support of MKE and KIAT through the Workforce Development Program in Strategic Technology and by Strategic Technology, and Basic Science Research Program through the National Research Foundation of Korea (NRF) funded by the Ministry of Education, Science and Technology (2009-0080273) to carry out this work was greatly acknowledged.

References

- [1] Chen CT. *Chem Mater* 2004;16:4389–440.
- [2] Kim YH, Kim HS, Lee KH, Kwon SK, Kim SH. *Mol Cryst Liq Cryst* 2006;444:257–63.
- [3] Yu MX, Chang LC, Lin CH, Duan JP, Wu FI, Chen IC, et al. *Adv Funct Mater* 2007;17:369–78.
- [4] Li J, Liu D, Hong Z, Tong S, Wang P, Ma C, et al. *Chem Mater* 2003;15:1486–90.
- [5] Wang P, Xie Z, Tong S, Wong O, Lee CS, Wong N, et al. *Chem Mater* 2003;15:1913–7.
- [6] Kang DM, Kang JW, Park JW, Jung SU, Lee SH, Park HD, et al. *Adv Mater* 2008;20:2003–7.
- [7] Park YS, Kang JW, Kang DM, Park JW, Kim YH, Kwon SK, et al. *Adv Mater* 2008;20:1957–61.
- [8] Hong ZR, Lee CS, Lee ST, Li WL, Liu SY. *Appl Phys Lett* 2003;82:2218–21.
- [9] Picciolo LC, Murata H, Kafafi ZH. *Appl Phys Lett* 2001;78:2378–81.
- [10] Hamada Y, Kanno H, Tsujioka T, Takahashi H, Usuki T. *Appl Phys Lett* 1999;75:1682–5.
- [11] Ning Z, Chen Zhao, Zhang Q, Yan Y, Qian S, Cao Y, et al. *Adv Funct Mater* 2007;17:3799–807.
- [12] Ning Z, Zhou Y, Zhang Q, Ma D, Zhang J, Tian H. *J Photochem Photobiol A: Chem* 2007;193:8–16.
- [13] Ju JU, Jung SO, Zhao QH, Kim YH, Je JT, Kwon SK. *Bull Korean Chem Soc* 2008;29:335–40.
- [14] Li SF, Zhong G, Zhu WH, Li FY, Pan JF, Huang W, et al. *J Mater Chem* 2005;15:3221–8.
- [15] Xu H, Yin K, Huang W. *Chem Eur J* 2007;13:10281–93.
- [16] Xu H, Wang LH, Zhu XH, Yin K, Zhong G, Hou XY, et al. *J Phys Chem B* 2006;110:3023–9.
- [17] Kido J, Okamoto Y. *Chem Rev* 2002;102:2357–67.
- [18] Huang TH, Lin JT. *Chem Mater* 2004;16:5387–93.
- [19] Tani K, Fujii H, Mao L, Sakurai H, Hirao T. *Bull Chem Soc Jpn* 2007;80:783–8.
- [20] Huang TH, Whang WT, Zheng HG, Lin JT. *J Chin Chem Soc* 2006;53:233–42.
- [21] Chang CY, Hsieh SN, Wen TC, Guo TF, Cheng CH. *Chem Phys Lett* 2006;418:50–3.
- [22] Chen S, Xu X, Liu Y, Yu G, Sun X, Qui W, et al. *Adv Funct Mater* 2005;15:1541–6.
- [23] Kim YH, Lee SJ, Jung SY, Byeon KN, Kim JS, Shin SC, et al. *Bull Korean Chem Soc* 2007;28:443–6.
- [24] Kim YH, Kwon SK, Yoo DS, Rubner MF, Wrighton MS. *Chem Mater* 1997;9:2699–701.
- [25] Kim YH, Shin DC, Kim SH, Ko CH, Yu HS, Chae YS, et al. *Adv Mater* 2001;13:1690–3.
- [26] Kim YH, Jung HC, Kim SH, Yang KY, Kwon SK. *Adv Funct Mater* 2005;15:1799–805.
- [27] Park JW, Kang PT, Park HT, Oh HY, Yang JW, Kim YH, Kwon SK. *Dyes and Pigments* 2010;85:93–8.
- [28] Park JW, Kim YH, Jung SY, Byeon KN, Jang SH, Lee SK, et al. *Thin Solid Films* 2008;516:8381–5.
- [29] So KH, Park HT, Shin SC, Lee SK, Lee DH, Lee KH, et al. *Bull Korean Chem Soc* 2009;30:1611.
- [30] Jo WJ, Kim KH, No HC, Shin DY, Oh SJ, Son JH, et al. *Synth Metal* 2009;159:1359–64.
- [31] Chang S, Ravi Shankar BK, Shechter H. *J Org Chem* 1982;47:4226–34.
- [32] Klingsberg E, Lewis CE. *J Org Chem* 1975;40:366–8.